JBC Papers in Press. Published on May 28, 2004 as Manuscript M312968200

Laboratory-Evolved Vanillyl-Alcohol Oxidase Produces Natural Vanillin

Robert H. H. van den Heuvel#¶, Willy A. M. van den Berg§, Stefano Rovida# and Willem J. H. van Berkel§*

From the #Department of Genetics and Microbiology, University of Pavia, via Abbiategrasso 207, 27100 Pavia, Italy, ¶Department of Biomolecular Mass Spectrometry, Bijvoet Center for Biomolecular Research and Utrecht Institute for Pharmaceutical Sciences, Utrecht University, 3584 CA Utrecht, The Netherlands and the §Laboratory of Biochemistry, Wageningen University, Dreijenlaan 3, NL-6703 HA Wageningen, The Netherlands

Running Title: Directed Evolution of Vanillyl-Alcohol Oxidase

*To whom correspondence should be addressed. Tel.: 31-317482861; Fax: 31-317-484801; E-mail: willem.vanberkel@wur.nl

The abbreviations used are: VAO, vanillyl-alcohol oxidase; PCMH, *p*-cresol methylhydroxylase; PCR, polymerase chain reaction.

Keywords: vanillyl-alcohol oxidase, random mutagenesis, directed evolution, substrate specificity, flavoenzyme, creosol, vanillin

Abstract

The flavoenzyme vanillyl-alcohol oxidase (VAO) was subjected to random mutagenesis to generate mutants with enhanced reactivity towards creosol (2-methoxy-4-methylphenol). The VAO-mediated conversion of creosol proceeds via a two-step process in which the initially formed vanillyl alcohol (4-hydroxy-3-methoxybenzyl alcohol) is oxidized to the widely used flavor compound vanillin (4-hydroxy-3-methoxybenzaldehyde). The first step of this reaction is extremely slow due to the formation of a covalent FAD (N5)-creosol adduct. After a single round of error-prone polymerase chain reaction, seven mutants were generated with an increased reactivity towards creosol. The single-point mutants Ile238Thr, Phe454Tyr, Glu502Gly and Thr505Ser showed an up to 40-fold increase in catalytic efficiency (k_{cat}/K_m) for creosol compared to wild-type enzyme. This enhanced reactivity was due to a lower stability of the covalent flavin-substrate adduct, thereby promoting vanillin formation. The catalytic efficiencies of the mutants were also enhanced for other *ortho*-substituted 4-methylphenols, but not for *p*-cresol (4-methylphenol). The replaced amino acid residues are not located within a distance of direct interaction with the substrate and the determined three-dimensional structures of the mutant enzymes are highly similar to wild-type enzyme. The present results clearly show the importance of remote residues, not readily be predicted by rational design, for the substrate specificity of enzymes.

Introduction

The increased use of enzymes and other proteins in the pharmaceutical, chemical and agricultural industry has generated considerable interest in the design of proteins with new or improved properties. Two different but complementary technologies have been applied to this goal: (i) rational design, which relies on the availability of the three-dimensional structure and knowledge about the relationship between sequence, structure and mechanism and (ii) directed evolution methods, which use random mutagenesis of the gene encoding the protein or recombination of gene fragments to create diversity and then experimentally screen the libraries generated for the desired properties. Rational design has been used to elucidate and change enzyme mechanism, substrate and product specificity, enantioselectivity, cofactor specificity and protein stability (1-3). Directed evolution has been applied to increase catalytic activity, invert or improve enantioselectivity, alter substrate and product specificity, protein stability, pH optimum and tolerance against organic solvents (1, 4-7). An obvious advantage of directed evolution methods over site-directed mutagenesis is that enzymes can be tailored for the production of (intermediate) products without detailed knowledge of protein structure and structure-function relationships.

In this study, we have engineered the flavoenzyme vanillyl-alcohol oxidase (VAO) by random mutagenesis such that the evolved mutants are capable of producing natural vanillin (4-hydroxy-3-methoxybenzaldehyde) from the precursor creosol (2-methoxy-4-methylphenol). Vanillin is a widely used flavor compound in food and personal products with an estimated annual worldwide consumption of over 2,000 tons (8,9). Moreover, vanillin displays antimicrobial and antioxidant properties and is used as a food preservative and for medicinal purposes (10-15). Natural vanilla flavor from the orchid *Vanilla planifolia* (16,17) supplies for less than 1% of the total demand for vanillin. Therefore, because of the increasing interest in natural products, alternative processes are being developed to produce natural vanillin (15, 18-20). One possible approach involves the use of enzymes such as vanillyl-alcohol oxidase (VAO) (21). This flavoprotein is able to produce vanillin from creosol (Fig. 1) and, if optimized for this purpose, would provide an attractive alternative for the production of the natural form of vanillin.

VAO is an oxidase from the ascomycete *Penicillium simplicissimum,* containing a covalently bound FAD cofactor. The enzyme is the prototype of a large family of structurally related oxidoreductases sharing a conserved FAD-binding domain (22,23). VAO catalyzes the oxidation of a wide range of phenolic compounds including 4-alkylphenols (24,25). The

catalytic cycle of VAO with 4-alkylphenols consists of two half-reactions (Fig. 1) (26,27). In the reductive half-reaction, FAD is reduced by the aromatic substrate with the concomitant formation of a *p*-quinone methide product intermediate. In the oxidative half-reaction, FAD is reoxidized and the *p*-quinone methide reacts with water to yield the corresponding 1-(4'-hydroxyphenyl)alcohol. The formed alcohol product can be further oxidized by VAO, via a similar mechanism, to 1-(4'-hydroxyphenyl)alkanone.

VAO has many properties in common with *p*-cresol methylhydroxylase (PCMH), a heterotetrameric flavocytochrome involved in the degradation of aromatic compounds in *Pseudomonas* species (28). The flavoprotein subunit of PCMH shares 32% sequence identity with VAO and their active sites are remarkably conserved. Superposition of the crystallographic models of VAO (accession code 1VAO) (23) and PCMH (accession code 1DIQ) (29) has revealed a root mean square (RMS) deviation of 1.0 Å for 470 Cα atoms. The two enzymes catalyze similar reactions but *p*-cresol (4-methylphenol), the physiological substrate of PCMH (30), is an extremely poor substrate for VAO (27). Kinetic studies have shown that the low activity of VAO with *p*-cresol, and also creosol, is due to the formation of an air-stable flavin (N5)-substrate adduct (21,27,31). From the available crystallographic data it is not obvious which structural features are involved in determining the different reactivity of both enzymes towards 4-methylphenols. The only non-conservative amino acid substitution in the active site is found near the reactive carbon atom of the substrate. This position is in VAO occupied by Thr457, whereas the equivalent residue in PCMH is Glu427. Studies from site-directed mutants have shown that residue 457 is not involved in the reactivity with 4-methylphenols (unpublished results), but is involved in determining the enantioselectivity of VAO (32).

In this contribution, we aimed to obtain, by directed evolution, VAO mutants with an enhanced reactivity towards creosol. To that end, we developed a library-screening assay for the production of vanillin and used error-prone polymerase chain reaction (PCR) to evolve VAO. Selected single-point mutant enzymes with improved reactivity towards creosol were characterized by kinetic studies and by X-ray crystallography.

Experimental Procedures

Chemicals, Bacterial Strains and Plasmids

Escherichia coli strain TG2 was used for both cloning and gene expression. Plasmid pUC19 was used for cloning and expression of the *vao* gene. Oligonucleotides, T4 DNA ligase, restriction enzymes, isopropyl β-D-thiogalactopyranoside, yeast extract and tryptone were from Life Technologies. Forward M13 and reverse M13 sequencing primers were from Amersham Biosciences. dNTP's and glucose oxidase (grade II) were purchased from Roche Applied Sciences and Taq DNA polymerase from HT Biotechnology. Eugenol (4-allyl-2-methoxyphenol), *p*-cresol, creosol, isoeugenol (2-methoxy-4-propenylphenol), 4-(methoxymethyl)phenol, vanillyl alcohol (4-hydroxy-3-methoxybenzyl alcohol), 2-amino-*p*-cresol, 2-methyl-*p*-cresol and 2-chloro-*p*-cresol were purchased from Aldrich.

Error-Prone PCR Mutagenesis

Plasmid pBC11 contains the *vao* gene with a silent mutation at position 882, introducing a *Sal*I restriction site (33). For random mutagenesis the *vao* gene in pBC11 was amplified using manganese-based error-prone PCR mutagenesis (34,35). A 25 µl volume PCR reaction mixture A containing 10 pmol of the primers 5'-GTAAAACGACGGCCAGT-3' and 5'-CAGGAAACAGCTATGAC-3', 90 ng template DNA and 250 or 500 pmol $MnCl_2$ was heated for 3 min at 95 ºC and, after cooling down to 80 ºC, mixed with 25 µl of mixture B containing 0.4 mM dATP and dGTP, 2 mM dCTP and dTTP, 2.5 U Taq DNA polymerase, 20 mM Tris/HCl (pH 8.85), 4 mM $MgCl_2$, 50 mM KCl, and 10 mM $(NH_4)_2SO_4$ in a thin-wall PCR tube. The thermal cycler performed 30 cycles with the following steps: 45 s at 94.5 ºC, 60 s at 48 ºC, and 120 s at 72 ºC. 2 µl of this PCR reaction was used in a second PCR reaction with the same set up except that $MnCl_2$ was exchanged with 2 nmol dITP. The final PCR products were digested with the restriction enzymes *Pst*I and *Kpn*I and the resulting fragments were subcloned into the corresponding sites of the pUC19 vector and transformed into *E. coli* TG2 cells by electroporation. The colonies were grown overnight on Luria-Bertani plates containing 100 µg/ml ampicillin at 37 ºC.

Preparation of Library, Screening and Enzyme Purification

Single colonies of transformed *E. coli* were transferred using a robotic system in 96-well plates (master plates) containing 200 µl Luria-Bertani medium and 100 µg/ml ampicillin.

After 48 hrs growth at 37 ºC and the addition of 10% (v/v) glycerine, the master plates were stored at -80 ºC. For screening, master plates were replicated into 96-well plates containing 200 µl Luria-Bertani medium, 100 µg/ml ampicillin and 20 µg/ml isopropyl β-D-thiogalactopyranoside. After 40 hrs of growth at 37 ºC, 50 µl aliquots of the cells were screened for creosol conversion at pH 8 and pH 10 and for vanillyl alcohol conversion at pH 8. The activity of the cells was measured by following absorption spectral changes due to the conversion of creosol and vanillyl alcohol into vanillin at 340 nm at a substrate concentration of 750 µM. Out of 9,600 clones seven clones with the highest activity towards creosol were selected and grown overnight at 37 ºC in 5 ml Luria-Bertani medium supplemented with 100 µg/ml ampicillin and 20 µg/ml isopropyl β-D-thiogalactopyranoside. Cells from the 5 ml culture were spun down and resuspended in 50 mM potassium phosphate buffer (pH 7.5). The cells were disrupted by sonication and the cell extract was collected after centrifugation. The activity of the cell extract towards creosol and vanillyl alcohol was measured as described below. Next, the cell extracts were analyzed by SDS-polyacrylamide gel electrophoresis and the amount of VAO in the cell extracts was estimated by comparing the fluorescence of the covalently bound FAD cofactor of VAO in the cell extracts with the fluorescence of known amounts of purified VAO in a gel incubated in 5% (v/v) acetic acid. The seven clones with the highest activity towards creosol were sequenced. Wild-type VAO and the mutants were overexpressed and purified according to a previously established procedure (33,36). The enzyme purity was checked by SDS-polyacrylamide gel electropheresis and by size-exclusion chromatography.

Analytical Methods

All experiments were performed in 50 mM potassium phosphate (pH 7.5) or glycine/potassium hydroxide (pH 10) at 25 ºC. SDS-polyacrylamide gel electrophoresis was carried out in 12.5 % slab gels essentially as reported earlier (37). Coomassie Brilliant Blue R-250 was used for protein staining. Before protein staining, gels were incubated in 5% (v/v) acetic acid for fluorescence detection of covalently bound FAD (38). Analytical size-exclusion chromatography was performed with a Superdex 200 PG 10/30 column (Amersham Biosciences) (27). Absorption spectra were recorded using a Hewlett-Packard HP 8453 diode-array spectrophotometer. Fluorescence spectra were recorded on a Cary Eclipse fluorescence spectrophotometer using an excitation wavelength of 360 nm. HPLC experiments were performed with an Applied Biosystems pump equipped with a Waters 996

photodiode-array detector and a 4.6 by 150 mm Alltech C18 column, essentially as reported previously (25).

VAO activity was routinely assayed by following absorption spectral changes of aromatic substrates. Initial rates were linear with enzyme concentration (50-1000 nM). Formation of 4-hydroxybenzaldehyde was measured at 330 nm (ε = 10.0 mM^{-1} cm^{-1} at pH 7.5 and ε = 25.6 mM^{-1} cm^{-1} at pH 10), formation of vanillin at 340 nm (ε = 14.0 mM^{-1} cm^{-1} at pH 7.5 and ε = 23.0 mM^{-1} cm^{-1} at pH 10), formation of 4-hydroxy-3-methoxycinnamyl alcohol at 296 nm for pH 7.5 (ε = 5.9 mM^{-1} cm^{-1}) and 290 nm for pH 10 (ε = 10.9 mM^{-1} cm^{-1}) and formation of 4-hydroxycinnamyl alcohol at 290 nm for pH 7.5 (ε = 3.4 mM^{-1} cm^{-1}) and at 314 nm for pH 10 (ε = 4.2 mM^{-1} cm^{-1}). Formation of 2-amino-4-hydroxybenzaldehyde and 2-methyl-4-hydroxybenzaldehyde was monitored at 340 nm. The molar absorption coefficients of 2-amino-4-hydroxybenzaldehyde and 2-methyl-4-hydroxybenzaldehyde were estimated on the basis of the molar absorption coefficient of vanillin and the yield of conversion using a known concentration of substrate (ε = 14 mM^{-1} cm^{-1} at pH 7.5 and ε = 24 mM^{-1} cm^{-1} at pH 10). The yield of conversion was estimated using HPLC product analysis. For enzyme-monitored-experiments, 8 μM enzyme and 200 μM air-saturated substrate were mixed and the redox state of the FAD cofactor was monitored continuously by diode-array absorption spectrophotometry.

Stopped-flow kinetics was performed with a Hi-Tech SF-51 apparatus equipped with a Hi-Tech SU-40 spectrophotometer (26). In anaerobic FAD reduction experiments, glucose-containing enzyme solutions were flushed with oxygen-free argon gas and glucose oxidase was added to eliminate final traces of oxygen.

For electrospray ionization mass spectrometry, VAO samples were prepared in 50 mM ammonium acetate (pH 6.8). Enzyme samples were introduced into the nanoflow electrospray ionization source of a Micromass LCT mass spectrometer (Waters), operating in positive ion mode. Source pressure conditions and electrospray voltages were optimized for transmission of larger VAO assemblies (Pirani pressure 6 mbar, capillary voltage 1450-1650 V and cone voltage 45-100) (39). Borosilicate glass capillaries (Kwik-Fil, World Precision Instruments) were used on a P-97 puller (Sutter Instruments) to prepare the nanoflow electrospray capillaries with an orifice of about 5 μM. The capillaries were subsequently coated with a thin gold layer (~500 Å) using an Edwards Scancoat six Pirani 501 sputter coater (Edwards High Vacuum International).

Crystallization and Structure Determination

Crystals of four VAO mutants were grown at 20 ºC by the hanging-drop vapor diffusion method. The drops contained 4 µl of an equal mixture of protein solution (6.5-13 mg/ml) in 50 mM potassium phosphate (pH 7.5) and reservoir solution containing 100 mM sodium acetate/hydrochloride (pH 5.1) and 4-6% (w/v) polyethylene glycol 4000. Hanging drops were allowed to equilibrate against 1 ml of reservoir solution for four days until yellow crystals appeared. Enzyme-inhibitor complexes were prepared by soaking the enzyme crystals in the reservoir solution containing 5 mM isoeugenol for one hour.

Diffraction data of the VAO mutant crystals were collected using a Rigaku R-AXIS IV image plate detector mounted on a RU-200B rotating anode Cu *K*α X-ray generator equipped with a MSC confocal optic system. VAO crystals were placed for a few seconds in a cryoprotectant solution containing sodium acetate/hydrochloride (pH 5.1), 4-6% (w/v) polyethylene glycol 4000 and 20% (v/v) glycerol. VAO crystals had the symmetry space group I4 and two molecules in the asymmetric unit. The data were processed with MOSFLM (40) and further processed with programs from the CCP4 package (41). Data processing statistics are reported in Table I. The mutant crystals are isomorphous to those of wild-type crystals. The final model of free wild-type VAO (accession code 1VAO) (23) was used as starting model for refinement of the evolved VAO mutants. The subsequent refinement of the initial model consisted of alternating rounds of manual fitting of the model to electron density maps using the program O (42) and maximum likelihood refinement with REFMAC (43). Five percent of the data were set aside to compute R_{free} (44). R_{free} was used to monitor the progress of the refinement. Refinement statistics are shown in Table I. The final models of the VAO mutants constist of two polypeptide chains with a total of 1098 residues (A6-A41, A47-A560, B6-B41, B47-B560), two FAD and two isoeugenol molecules.

Results

Directed Evolution of VAO and Characterization of Mutant Enzymes

Random mutations were introduced into the *vao* wild-type gene coding for 560 amino acids by error-prone PCR. We used manganese concentrations designed to generate 1-4 mutations per *vao* gene to produce an average of one amino acid substitution per VAO molecule (45). Sequence determination of 42 randomly picked colonies showed that the evolved mutations were divided equally over the *vao* gene, however, we found more A and T mutations (70% of total) than G and C mutations (30% of total). After one round of mutagenesis, the activity of the clones towards creosol was determined at pH 8 and 10 at saturating substrate concentrations. The molar absorption coefficient of vanillin at pH 8 and 10 is 16.0 and 23.0 mM^{-1} cm^{-1}, respectively. From 9,600 clones we selected seven clones with an increased reactivity towards creosol (Table II). Sequencing revealed that three mutant enzymes shared the amino acid substitution Ile238Thr, whereas all other mutations were found only once. The turnover rate at pH 10 in the cell extracts of five single mutants, one double mutant and one triple mutant was 4-7-fold higher compared to wild-type enzyme (Table II).

To study the rational for the increased reactivity towards creosol we proceeded with the four single-point mutants Ile238Thr, Phe454Tyr, Glu502Gly and Thr505Ser. These mutants were overexpressed in *E. coli*, purified and analyzed in detail. The evolved mutants were, like wild-type VAO, expressed to about 2.5% of total protein in *E. coli* strain TG2. The purified enzymes were bright yellow and enzyme purity was higher than 95% as estimated by SDS-polyacrylamide gel electropheresis. Size-exclusion chromatography revealed that the mutant enzymes were, as wild-type enzyme, in equilibrium between dimeric and octameric forms (38). Next, we studied the hydrodynamic behavior of the VAO variants at low enzyme concentrations (1 and 4 μM) by electrospray mass spectrometry. The resulting data showed that Phe454Tyr and Thr505Ser VAO have a similar hydrodynamic behavior as wild-type enzyme (39). The most abundant species were found to be the octameric assembly with lower amounts of dimeric assembly (ratio octamer-dimer was about 1.5:1 for Phe454Tyr, Thr505Ser and wild-type VAO). The quaternary structures of Ile238Thr and Glu502Gly were different from wild-type enzyme. Ile238Thr appeared to be mainly present in the octameric form (ratio octamer-dimer 4:1) and Glu502Gly was almost completely present as a dimer (ratio octamer-dimer 1:10).

X-ray crystallography has shown that VAO His422 is covalently linked to the FAD prosthetic group via a FAD (C8α)-His422 (NE3) bond (23). Fluorescence analysis of unstained SDS-polyacrylamide gels in 5% (v/v) acetic acid showed that the four mutants were as fluorescent as wild-type enzyme, strongly indicating that the FAD is covalently bound to His422 in all four mutants.

The flavin absorption spectral properties of the VAO mutants were virtually identical to wild-type enzyme with maxima at 355 nm and 439 nm for Ile238Thr, Phe454Tyr and Thr505Ser and 357 nm and 442 nm for Glu502Gly (356 nm and 439 nm for wild-type enzyme). Moreover, the absorption ratio between 280 nm and 439 nm for the mutants was similar to the reported value (12.0-12.5) for wild-type VAO.

Catalytic Properties of VAO Mutants

The four purified VAO mutants were selected on the basis of their reactivity towards creosol. Table III (pH 7.5) and Table IV (pH 10) shows that the catalytic efficiencies (defined as k_{cat}/K_m) of the four mutants for this substrate were indeed 4-11-fold at pH 7.5 and 20-40-fold at pH 10 higher than that of wild-type VAO. The increased catalytic efficiency was mainly due to an increase in turnover rate and not due to a lowered Michaelis constant. This is in agreement with the screening procedure in which we used saturating substrate conditions of 750 μM creosol. Apart from the enhanced reactivity towards the substrate for which was screened for, the evolved mutant enzymes had remarkably different catalytic properties than wild-type VAO (Table III and IV). The *ortho*-substituted 4-methylphenol derivatives 2-methyl-*p*-cresol and 2-amino-*p*-cresol were converted with higher catalytic efficiencies than wild-type VAO, especially at pH 10. 2-Chloro-*p*-cresol on the other hand, was neither a substrate for the mutants nor for wild-type VAO. *p*-Cresol, the physiological substrate of PCMH, is a very poor substrate for VAO (27). Intriguingly, the mutant enzymes performed worse than wild-type VAO with this substrate (turnover rates lower than 0.001 s^{-1}). It should be stressed here that the investigated 4-methylphenol derivatives react, unlike other VAO substrates, via a two-step reaction to the corresponding aldehyde (Fig. 1) and that the steady-state kinetic assay only monitored the production of the aldehyde.

Like wild-type VAO, the evolved mutants had a relaxed substrate specificity towards other 4-hydroxybenzylic compounds (24,25). Since vanillyl alcohol is the intermediate product formed upon hydroxylation of creosol it was of special interest to study the reactivity of the mutant enzymes with this substrate. The catalytic efficiencies at both pH 7.5 and pH 10 with

vanillyl alcohol were similar compared with wild-type VAO, despite a considerably lower maximum turnover rate (Table III and IV). The supposed physiological substrate 4-(methoxymethyl)phenol (26) was oxidized efficiently by the mutant enzymes. In fact, the catalytic efficiencies at pH 10 with this substrate were 4-9-fold higher compared to wild-type enzyme (Table IV). As 4-allylphenols are among the best substrates for VAO (24) it was also of interest to study reactivity of the mutant enzymes with eugenol. At pH 7.5, wild-type VAO converted eugenol to coniferyl alcohol (4-hydroxy-3-methoxycinnamyl alcohol) with a far higher catalytic efficiency than the mutants (10-250-fold), which was mainly caused by dramatically decreased turnover rates (Table III). At pH 10, however, wild-type VAO and Ile238Thr showed similar catalytic efficiencies with eugenol, although the maximum turnover rate of Ile238Thr was 65-fold lower than of wild-type enzyme (Table IV). The other three mutants displayed lower catalytic efficiencies with eugenol, which was, again, caused by strongly decreased turnover rates. In summary, the catalytic efficiency of the evolved VAO mutants was significantly increased towards *ortho*-substituted 4-methylphenols. However, the reactivity towards *p*-cresol and eugenol was decreased by the mutations.

Reduction of wild-type VAO (VAO_{ox}) in an anaerobic environment by 4-(methoxymethyl)phenol (S) results in a stable complex between reduced enzyme and the *p*-quinone methide of the substrate (VAO_{red}:Q), which is described by the following equation:

$$VAO_{ox} + S \underset{k_{-1}}{\overset{k_1}{\rightleftarrows}} VAO_{ox}{:}S \underset{k_{-2}}{\overset{k_2}{\rightarrow}} VAO_{red}{:}Q \qquad (1)$$

Under anaerobic conditions at pH 7.5, wild-type VAO is reduced by 4-(methoxymethyl)phenol in a single irreversible step (k_2 = 3.3 s^{-1} at saturating substrate conditions). The rate of reduction equals the maximum turnover rate of wild type VAO with this substrate (26). Anaerobic stopped-flow experiments showed that 4-(methoxymethyl)phenol-mediated reduction of the four VAO mutants also occurred in a single exponentional process with the formation of a stable complex between reduced enzyme and *p*-quinone methide intermediate. With all mutants, the rates of reduction at saturating substrate concentrations and pH 7.5 were in the same range as the turnover rates (k_2 = 2.9 s^{-1} for Ile238Thr, k_2 = 1.9 s^{-1} for Phe454Tyr, k_2 = 2.0 s^{-1} for Glu502Gly and k_2 = 2.5 s^{-1} for Thr505Ser), suggesting that the mutant enzymes have the same mechanism of action with 4-(methoxymethyl)phenol as wild-type enzyme.

Reduction of VAO by creosol can also be described by the above equation, however, with this substrate the reductive half-reaction does not limit catalysis (21). Table V summarizes the data of the reductive half-reaction of wild-type VAO and the mutants by creosol at pH 7.5 and pH 10. When creosol was mixed with wild-type VAO, the FAD cofactor reduced in a single exponentional step. However, when the kinetic data were analyzed, a best fit was obtained when an apparent 'initial' reduction rate at infinite low substrate concentration was taken into account (45):

$$k_{obs} = \frac{k_1 * k_2 * [S]}{k_1 * [S] + k_{-1}} + k_{-2}; \qquad k_{-1}/k_1 = K_d \qquad (2)$$

This suggests that the reduction process was reversible ($k_{-2} > 0$) and that the creosol-mediated reduction of the FAD cofactor resulted in an equilibrium in which the flavin is partially in the oxidized state. The rate of enzyme reduction was dependent on the substrate concentration with a dissociation constant (k_{-1}/k_1) of 188 μM at pH 7.5. At low creosol concentrations the reduction rate reached the finite value 0.18 s^{-1} (k_{-2}). The reduction rate at saturating substrate concentration was calculated to be 0.57 s^{-1} (k_2) and was 29-fold higher than the turnover rate, which indicates that the reduction rate does not determine the rate of overall catalysis. Like with wild-type enzyme, the creosol-mediated reduction of the mutants was best described by a reversible reduction process. The maximum reduction rates of Phe454Tyr (k_2 = 0.25 s^{-1}) and Thr505Ser (k_2 = 0.36 s^{-1}) with creosol at pH 7.5, however, were in the same order of magnitude as their turnover rates (k'_{cat} = 0.14 s^{-1} and k'_{cat} = 0.12 s^{-1}, respectively), suggesting that the reduction may partially limit catalysis at neutral pH (Fig. 2). The calculated reverse reduction rates of the mutants were comparable with wild-type VAO (k_{-2} = 0.24 s^{-1} and k_{-2} = 0.18 s^{-1} for Phe454Tyr and Thr505Ser, respectively). The reduction rates of the mutant enzymes with creosol increased with pH and became far higher than the turnover rates (Table V). Thus, at basic pH values the reduction rate does not limit catalysis for wild-type VAO, Phe454Tyr and Thr505Ser.

FAD-Substrate Adduct in VAO Mutants

Enzyme-monitored-turnover experiments and fluorescence spectroscopy have indicated that the FAD cofactor of wild-type VAO forms covalent flavin N5 adducts with both *p*-cresol and creosol, and that these adducts become more stable at higher pH (21,27). Because the evolved

VAO mutants, especially at basic pH values, converted creosol to vanillin much better than wild-type enzyme, it was of interest to investigate adduct formation with the mutant enzymes with these techniques. In enzyme-monitored-turnover experiments it was found that at neutral pH the FAD in wild-type VAO and Glu502Gly was for 47% and 45%, respectively, in the oxidized state (Table VI). On the other hand, the FAD in Ile238Thr, Phe454Tyr and Thr505Ser was for more than 50% in the oxidized state. This suggests that in the latter three mutants the covalent adduct was less stabilized than in wild-type VAO and the Glu502Gly variant. At pH 10, the differences in the FAD redox state between wild type VAO and the four mutants became more pronounced. Under these conditions, the relative amount of oxidized FAD in the four mutants was 2-3-fold larger than in wild type enzyme, indicative for a lower stability of the adduct (Table VI).

When adduct formation between protein-bound FAD and creosol was studied by fluorescence spectroscopy, mixing of (mutant) enzyme and substrate at pH 7.5 resulted in the initial formation of an emission spectrum with a maximum at 480 nm. This spectrum, indicative for the flavin (N5)-creosol adduct (21), was stable for a few minutes after which it changed to a spectrum with an emission maximum at 425 nm (Fig. 3). The latter spectrum represented vanillin, the fluorescent end product of the two-step oxidation of creosol. For both wild-type VAO and the mutants the covalent flavin N5-substrate adduct became more stable at pH 10 (Fig. 3), in good agreement with the apparent reduced state of the flavin cofactor observed during enzyme-monitored-turnover experiments. However, as at pH 7.5, the adduct decay was much faster in the mutant enzymes.

When adduct formation between the mutant enzymes and *p*-cresol was studied at pH 7.5 and 10 we observed fluorescence spectra with very stable emission maxima at 480 nm, indicating the formation of abortive FAD (N5)-*p*-cresol adducts. As for wild type VAO, the FAD (N5)-*p*-cresol adduct was stable for several minutes (27). In summary, enzyme-monitored-turnover and fluorescence emission experiments showed that the four single-point mutations decreased the stability of the covalent adduct between the FAD cofactor and creosol, however, the four mutations did not have an effect on the stability of the flavin adduct formed in the reaction with *p*-cresol. These data agree well with the kinetic data (Table III and IV).

Crystal Structures of VAO Mutants

The crystal structures of the evolved mutants Ile238Thr, Phe454Tyr, Glu502Gly and Thr505Ser, refined to a resolution of 2.55 Å, 2.7 Å, 3.0 Å and 2.7 Å, respectively, are highly

similar to wild-type VAO (Table I). The present medium-resolutions, however, do not allow the identification of very subtle structural perturbations due to the mutations. The RMS deviation between the wild-type enzyme and Ile238Thr, Phe454Tyr, Glu502Gly, and Thr505Ser is 0.24 Å, 0.26 Å, 0.33 Å, and 0.27 Å, respectively. The electron densities of the structures of the mutant enzymes clearly confirmed the substitution of the different amino acids and the presence of the inhibitor isoeugenol. Fig. 4 displays the position of the four amino acid replacements in the VAO monomer.

Residue Ile238 is positioned in a short α-helix in the FAD-binding domain at the interface between two VAO monomers. The introduction of Thr238 did not have any effect on the conformation in the region around residue 238 in both monomers. Moreover, compared to the native model, no conformational shifts were found in the position of isoeugenol, FAD or the residues lining the enzyme active site. Like in wild-type VAO (23), the aromatic ring of the substrate analog isoeugenol stacks against the isoalloxazine ring of FAD at an angle of 14 degrees with respect to the cofactor plane. The hydroxyl moiety of isoeugenol forms a hydrogen bond with the side chains of Tyr108, Tyr503, and Arg504, facilitating substrate deprotonation, and the propenyl group points towards Asp170. The Cα atom of the propenyl group is positioned at 3.4 Å from flavin N5.

Residue Phe454 is situated in a loop, deeply buried within the cap domain. The Phe454Tyr mutation does not introduce any shifts within the region around Tyr454 nor in the VAO active site cavity and the orientation of bound isoeugenol (Fig. 5A). The extra hydroxyl group introduced by Tyr454 potentially forms an additional hydrogen bond with the NE2 atom of His467, which together with its neighbor His466 forms part of the active site of VAO.

Glu502 and Thr505 are positioned in the FAD-binding domain in a loop close to the active site cavity of VAO. In fact, the neighboring residues Tyr503 and Arg504 stabilize the phenolate form of the substrate by forming hydrogen bond interactions (23). The two mutations Glu502Gly and Thr505Ser did not induce any major conformational changes in this loop or the side chains of Tyr503 or Arg504 (Fig. 5B). However, the Glu502Gly mutation has an effect on the hydrogen bond network as two potential hydrogen bond interactions between the negatively charged side chain of Glu502 and the carbonyl oxygens of Arg504 and Ser426 cannot be formed.

Discussion

The structurally related flavoenzymes VAO and PCMH have many catalytic properties in common but show dramatic differences in their performance towards 4-methylphenols. Of special interest is the production of the widely used flavor compound vanillin from the natural precursor creosol. Because PCMH is highly active with creosol and VAO is not, we undertook the enhancement of the reactivity of VAO with creosol by manganese-based error-prone PCR.

The key factor for a successful random mutagenesis experiment is a rapid and effective screening or selection procedure (47). Chromogenic substrates have been used successfully in a number of studies utilizing a 96-well plate reader or visual screening of the colored colonies (48,49). With VAO, the end product vanillin formed upon the two-step oxidation of creosol could be measured directly in whole cells by absorption spectroscopy at 340 nm. Both creosol and vanillin are able to diffuse efficiently through the *E. coli* membrane such that vanillin is produced in the intracellular environment and is monitored in the extracellular environment. The evolved VAO mutants were selected on the basis of their reactivity towards creosol at both pH 8 and 10. With this screening procedure, we found seven clones with a considerably increased reactivity towards creosol. Interestingly, none of the mutations was positioned within a distance of direct interaction with the substrate. The Ile238Thr mutation was found three times, whereas the other mutations, Phe454Tyr, Glu502Gly and Thr505Ser, were found only once. The high frequency of the Ile238Thr mutation was not due to sequence bias as proven by sequence determination of randomly picked colonies. On the basis of the mutational efficiency, this residue could have been replaced by several other residues, however, only the Ile238Thr mutation was detected. This indicates that position 238 is a hot spot in determining the reactivity towards *ortho*-substituted 4-methylphenols.

Previous studies have shown that the poor reactivity of VAO towards creosol is due to the formation of an abortive covalent FAD (N5)-creosol adduct (21,27). Adduct formation was less favorable in the here presented mutant enzymes, resulting in considerably increased conversion rates, especially at basic pH values. Similar effects were observed with other *ortho*-substituted 4-methylphenol substrates and rate enhancements of up to 80-fold occurred. The mutant enzymes had a relaxed specificity towards other 4-hydroxybenzylic compounds, but the maximum turnover rates and the Michaelis constants for the various substrates varied among the different mutants and wild-type enzyme (Table III and IV).

Intriguingly, *p*-cresol was, as for wild-type VAO, a very poor substrate for the generated mutants. Indeed, the mutants formed a very stable covalent flavin-*p*-cresol adduct, thereby preventing product formation. The X-ray model of wild-type VAO in complex with *p*-cresol has shown that formation of the flavin adduct is associated with a distortion of the FAD ring, which deviates from planarity with an angle of 8 degrees between the pyrimidine and dimethylbenzene rings. Moreover, *p*-cresol makes an angle of 34° with the flavin whereas the non-covalently bound inhibitors isoeugenol and 2-nitro-*p*-cresol are less tilted with respect to the FAD. From this it was argued that steric restrictions imposed by the shape of the active site cavity are a key factor for preventing enzyme inactivation through covalent adduct stabilization (23). The X-ray models of Ile238Thr, Phe454Tyr, Glu1502Gly and Thr505Ser did not reveal any conformational perturbations in the active site cavities and the orientation of the flavin and isoeugenol were highly conserved. In addition, the X-ray models did not suggest structural perturbations in regions far from the catalytic center. It should be stressed, however, that the medium-resolution (2.55-3.0 Å) of the presented X-ray structures is not sufficient to detect very subtle perturbations. This conservation of structural features might explain why all mutant enzymes formed very stable flavin-*p*-cresol adducts. However, the structural data do not provide us with a clue why only wild-type enzyme forms a stable adduct with creosol.

The active site topology of VAO is highly similar to that of PCMH with several conserved key residues (Fig. 5C) (29). The closest distance between *p*-cresol (C7) and FAD (N5) in the PCMH crystallographic model is 3.1 Å and the orientation of the phenolic ring of the PCMH substrate is similar to that of the non-covalent phenolic inhibitors of VAO. Tyr108, Tyr503 and Arg504 in VAO (Tyr95, Tyr473 and Arg474 in PCMH) are involved in the deprotonation of the substrate phenol. Arg504/Arg474 are also proposed to stabilize the anionic form of the reduced FAD. As suggested for His436, Glu177 and Asp434 in PCMH (29), His466, Asp192 and Glu464 in VAO may form a proton transfer pathway during the formation of the quinone methide intermediate product. The most significant difference between the active sites of VAO and PCMH is the arrangement of acidic residues. Asp170 of VAO has no counterpart in PCMH but its role is taken over by Glu380. Furthermore, PCMH has a second acidic residue (Glu427) within the active site cavity, which is not present in VAO (Thr457). Previously, we have undertaken the assessment to mimic the active site of PCMH by creating the VAO double mutant Asp170Glu/Thr457Glu, however, these mutations do not have an effect on the tendency of VAO to form adducts with

4-methylphenols (32). Thus, the comparison of VAO with PCMH does not rationalize the adduct formation of VAO with *p*-cresol and creosol.

The kinetic and structural data presented in this paper clearly show that residues distal from the active site determine the reactivity towards creosol. This is in line with recent studies (5, 50-53), which indicate that enzymes exert their functions not only through the chemical properties of the side chains of the amino acid residues that contact the cofactor or the substrate, but also through long-range effects such as hydrogen bond networks and electrostatic interactions.

The Ile238Thr mutation was found in three of seven mutants with enhanced reactivity towards creosol. Ile238 is positioned at the VAO monomer-monomer interface at a distance of 33 Å from the FAD (N5). The Ile238Thr mutation does not induce any major structural change and neither prevents octamerization. This implies that a residue very far from the active site cavity without any apparent catalytic function plays a role in VAO catalysis. Intriguingly, the counterpart of this residue in PCMH is Thr207 (29), which is also positioned at the monomer-monomer interface.

Phe454 is also positioned far (16 Å) from the FAD (N5), but is localized within the cap domain. The Phe454Tyr mutation is conserved in PCMH (Tyr424). The hydroxy moiety of the Tyr454 side chain is hydrogen bonded to the strictly conserved His467 (His437 in PCMH), which is pointing towards the active site cavity and the FAD cofactor (Fig. 5A). In fact, the neighboring residue His466 is lining the active site cavity of VAO. This suggests that the Phe454Tyr mutation might influence catalysis by introducing subtle changes in electrostatic interactions and possible backbone flexibility. We have no indication that Tyr454 and His467 are involved in an extended hydrogen bond network.

Both Glu502 and Thr505 are positioned in a loop lining the VAO catalytic center and are in relatively short distance from FAD (N5): 11.8 Å for OE2 of Glu502 and 12.4 Å for CA of Thr505. The generated mutations at these positions (Glu502Gly and Thr505Ser) are not conserved in PCMH (Val472 and Val475). Due to the Glu502Gly mutation a negative charge near the enzyme catalytic center is removed as well as two possible hydrogen bond interactions between the side chain of Glu502 and the carbonyl oxygens of Arg504 and Ser426. The Thr505Ser mutation has no effect on neighboring hydrogen bond interactions. It should be mentioned here that the active site cavity of VAO is completely solvent inaccessible (23). Close inspection of the VAO X-ray model does not suggest an obvious structural element, whose conformational change may allow substrate admission. This

implies that the substrate enters the active site cavity by 'breathing' of the enzyme. We speculate that this property of VAO is somewhat changed in the evoluted mutants.

In conclusion, we created by error-prone PCR four single-point mutants distal from the VAO active site cavity with an enhanced reactivity towards creosol and other *ortho*-substituted 4-methylphenols. Given the small differences in structural properties we are not able to offer a clear explanation for the different activity changes encountered with different substrates. Nevertheless, our results demonstrate the power of directed evolution to generate mutations that would not readily predicted by site-directed mutagenesis. Moreover, we confirm earlier findings that changing enzyme activity requires not only remodeling of the active site cavity by mutations of residues within the active site pocket, but also by distal mutations. The results obtained in this study with single-point mutations can serve as a starting point to investigate possible cumulative effects of residues remote from the active site cavity by performing successive rounds of error-prone PCR. An interesting approach to investigate possible long-range structural perturbations in VAO (not detected in the present study) is by the characterization of single and double mutants of two mutations that are known to have a stimulating effect on creosol reactivity, e.g Thr207Ser and Glu502Gly in VAO. In the case of structural perturbations caused by the single mutations, it is likely that the effect of the double mutation is nonadditive due to different structural perturbations. This principle has been demonstrated for some residues of dihydrofolate reductase (53,54).

Acknowledgments—We thank Andrea Mattevi for valuable discussions and Lisette Deddens for excellent mass spectrometry assistance. R. H. H. van den H. was supported by a Madam Curie Fellowship (HPMF-CT-2000-00786) from the European Community.

References

1. Bornscheuer, U. T., and Pohl, M. (2001) *Curr. Opin. Chem. Biol*. **5**, 137-143
2. Cedrone, D., Menze, A., and Quemeneur, E. (2000) *Curr. Opin. Struct. Biol*. **10**, 405-410
3. Regan, L. (1999) *Curr. Opin. Struct. Biol*. **9**, 494-499
4. Arnold, F. H. (1998) *Acc. Chem. Res*. **31**, 125-131
5. Oue, S, Okamoto, A., Yano, T., and Kagamiyama, H. (1999) *J. Biol. Chem*. **274**, 2344-2349
6. Schmidt-Dannert, C. (2001) *Biochemistry* **40**, 13125-13136
7. Tao, H., and Cornish, V. (2002) *Curr. Opin. Chem. Biol*. **6**, 858-864
8. Dignum, M. J. W., Kerler, J., and Verpoorte, R. (2001) *Food Rev. Int.* **17**, 199-219
9. Rao, S. R., and Ravishankar, G. A. (2000) *J. Sci. Food Agric*. **80**, 289-304
10. Aruoma, O. I. (1999) *Free Radic. Res*. 30, 419-427
11. Burri, J., Graf, M., Lambelet, P., and Löliger, J. (1989) *J. Agric. Food Chem*. **48**, 49-56
12. Cerrutti, P., Alzamora, S. M., and Vidales, S. L. (1997) *J. Sci. Food Agric*. **48**, 49-56
13. Fitzgerald, D. J., Stratford, M., and Narbad, A. (2003) *Intl. J. Food Microbiol*. **86**, 113-122
14. Kamat, J. P., Ghosh, A., and Devasagayam, T. P. (2000) *Mol. Cell. Biochem*. **209**, 47-53
15. Walton, N. J., Mayer, M. J., and Narbad, A. (2003) *Phytochemistry* **63**, 505-515
16. Bensaid, F., Wietzerbin, K., and Martin, G. J. (2002) *J. Agric. Food Chem*. **50**, 6271-6275
17. Podstolski, A., Havkin-Frenkel, D., Malinowski, J., Blount, J. W., Kouteva, G., and Dixon, R. A. (2002) *Phytochemistry* **61**, 611-620
18. Hagedorn, S., and Kaphammer, B. (1994) *Annu. Rev. Microbiol*. **48**, 773-800
19. Priefert, H., Rabenhorst, J., and Steinbüchel, A. (2001) *Appl. Microbiol. Biotechnol.* **56**, 296-314
20. Walton, N. J., Narbad, A., Faulds, C. B., and Williamson, G. (2000) *Curr. Opin. Biotechnol*. **11**, 490-496
21. Van den Heuvel, R. H. H., Fraaije, M. W., Laane, C., and van Berkel, W. J. H. (2001) *J. Agric. Food Sci.* **49**, 2954-2958

22. Fraaije, M. W., van Berkel, W. J. H., Benen, J. A. E., Visser, J., and Mattevi, A. (1998) *Trends Biochem. Sci.* **23**, 206-207
23. Mattevi, A., Fraaije, M. W., Mozzarelli, A., Olivi, L., Coda, A., and van Berkel, W. J. H. (1997) *Structure* **5**, 907-920
24. Fraaije, M. W., Veeger, C., and van Berkel, W. J. H. (1995) *Eur. J. Biochem.* **234**, 271-277
25. Van den Heuvel, R. H. H., Fraaije, M. W., and van Berkel, W. J. H. (1998) *J. Bacteriol.* **180**, 5646-5651
26. Fraaije, M. W., and van Berkel, W. J. H. (1997) *J. Biol. Chem.* **272**, 18111-18116
27. Fraaije, M. W., van den Heuvel, R. H. H., Roelofs, J. C. A. A., and van Berkel, W. J. H. (1998) *Eur. J. Biochem.* **253**, 712-719
28. Hopper, D. J. (1976) *Biochem. Biophys. Res. Commun.* 69, 462-468
29. Cunane, L. M., Chen, Z.-W., Shamala, N., Mathews, F. S., Cronin, C. N., and McIntire, W. S. (2000) *J. Mol. Biol*. **295**, 357-374
30. McIntire, W., Hopper, D. J., Craig, J. C., Everhart, E. T., Webster, R. V., Causer, M. J., and Singer, T. P. (1984) *Biochem. J.* **224**, 617-621
31. Van den Heuvel, R. H. H., Fraaije , M. W., and van Berkel, W. J. H. (2000) *FEBS Lett.* **481**, 109-112
32. Van den Heuvel., R. H. H., Fraaije, M. W., Ferrer, M., Mattevi, A., and van Berkel, W. J. H. (2000) *Proc. Natl. Acad. Sci. U. S. A*. **97**, 9455-9460
33. Van den Heuvel, R. H. H., Fraaije, M. W., Mattevi, A., and van Berkel, W. J. H. (2000) *J. Biol. Chem.* **274**, 14799-14808
34. Joo, H., Lin, Z., and Arnold, F. H. (1999) *Nature* **399**, 670-673
35. Lin-Goerke, L. J., Robbins, D. J., and Burczak, D. J. (1997) *Biotechniques* 23, 409-412
36. Benen, J. A. E., Sanchez-Torres, P., Wagemaker, M. J. HM., Fraaije, M. W., van Berkel, W. J. H., and Visser, J. (1998) *J. Biol. Chem*. **273**, 7865-7872
37. Laemmli, U. K. (1970) *Nature 227*, 680-685
38. Fraaije, M. W., Mattevi., A., and van Berkel, W. J. H. (1997) *FEBS Lett*. **402**, 33-35
39. Tahallah, N., van den Heuvel, R. H. H., van den Berg, W. A. M., Maier, C. S., van Berkel, W. J. H., and Heck, A. J. R. (2002) *J. Biol. Chem*, **277**, 36425-36432
40. Leslie, A. G. (1999) *Acta Crystallogr. Sect. D-Biol. Crystallogr.* **55**, 1696-1702
41. CCP4 (Computational Project Number 4) (1994) *Acta Crystallogr. Sect. D-Biol. Crystallogr.* **50**, 760-767

42. Jones, T. A., Zou, J. Y., Cowan, and S. W., Kjeldgaard, M. (1991) *Acta Crystallogr. Sect. A*. **47**, 110-119
43. Murshudov, G. N., Vagin, A. A., and Dodson, E. J. (1997) *Acta Crystallogr. Sect. D-Biol. Crystallogr.* **53**, 240-255
44. Brünger, A.T. (1992) *Nature* **355**, 472-475
45. Kuchner, O., and Arnold, F. H. (1997) *Trends Biotechnol*. **15**, 523-530
46. Strickland, S., Palmer, G., and Massey, V. (1975) *J. Biol. Chem.* **250**, 4048-4052
47. Zhao, H., and Arnold, F. H. (1997) *Curr. Opin. Struct. Biol*. **7**, 46-52
48. Moore, J. C., and Arnold, F. H. (1996) *Nat. Biotechnol*. **14**, 458-467
49. Zhang, J.-H., Dawes, G., and Stemmer, W. P. C. (1997) *Proc. Natl. Acad. Sci. U. S. A*. **94**, 4504-4509
50. Benkovic, A. J., and Hammer-Schiffer, S. (2003) *Science* **301**, 1196-1202
51. Liebeton. K., Zonta, A., Schimossek, k., Nardini, M., Lang, D., Dijkstra, B. W., Reetz, M. T., and Jaeger, K.-E. (2000) *Chem. Biol*. **7**, 709-718
52. Rajagopalan, P. T. R., Lutz, S., and Benkovic, S. J. (2002) *Biochemistry* **41**, 12618-12128
53. Rod, T. H., Radkiewicz, J. L., and Brooks, C. L. (2003) *Proc. Natl. Acad. Sci. U. S. A.* **100**, 6980-6985
54. Brown, K. A., Howell, E. E., and Kraut, J. (1993) *Proc. Natl. Acad. Sci. U. S. A.* **90**, 1753-11756
55. Laskowski, R. A., MacArthur, M. W., Moss, D. S., and Thornton, J. M. (1993) *J. Appl. Crystallogr.* **26**, 283-291
56. Kraulis, P. J. (1991) *J. Appl. Crystallogr.* **24**, 946-950
57. Merritt, E. A., and Bacon, D. J. (1997) *Methods Enzymol*. **277**, 505-524

Table I X-ray data collection and refinement statistics.

	Ili238Thr	Phe454Tyr	Glu502Gly	Thr505Ser
Data collection				
resolution range (Å)	40-2.55	40-2.7	40-3.0	40-2.7
cell parameters	$a = b = 129.90$, $c = 133.38$	$a = b = 129.90$, $c = 133.61$	$a = b = 129.91$, $c = 134.43$	$a = b = 129.52$, c = 133.28
observed reflections	252,743	161,609	239,148	185,245
unique reflections	35,898	30,132	22,257	29,902
completeness (%)[a]	98.9 (98.1)	97.7 (94.6)	97.6 (95.4)	97.9 (97.6)
R_{merge}[a,b]	7.9 (33.1)	8.8 (38.8)	12.7 (32.0)	7.5 (34.1)
intensities (I/σ)[a]	8.2 (2.1)	6.9 (1.9)	4.4 (1.9)	8.1 (1.9)
Refinement				
R_{factor}	20.7	20.3	21.7	20.7
R_{free}	27.2	29.3	30.7	29.2
no. atoms	8,828	8,832	8,820	8,828
no. of isoeugenol atoms	22	22	22	22
water molecules	0	0	0	0
RMS bond length	0.015	0.014	0.014	0.014
RMS bond angle	1.52	1.57	1.67	1.50
Ramachandran plot (%)[d]	87.1/12.9/0/0	85.8/14.1/0.1/0	82.0/17.7/0.3/0	85.1/14.7/0.2/0

[a] Numbers in parentheses corresponds to data in the outermost resolution shell.

[b] $R_{merge} = \sum |I_j - \langle I_j \rangle| / \sum \langle I_j \rangle$, where I_j is the intensity of an observation of reflection $_j$ and $\langle I_j \rangle$ is the average intensity for reflection $_j$.

[c] $R_{factor} = \sum |F_{obs}| - |F_{calc}| / \sum F_{obs}$, R_{free} for 5 % subset of reflections not included in the refinement (44).

[d] Percentages of residue in most favored, allowed, generously allowed and disallowed regions of the Ramachandran plot (55).

Table II Amino acid substitutions in VAO mutants and the turnover rates with creosol at pH 8 and pH 10 at 25 ºC.

Clone id.	k' (s^{-1}) pH 8[a]	k' (s^{-1}) pH 10[a]								
508E4	0.015	0.021			I238T		M437L			
531C7	n.d.	0.019	F93Y	P189S	I238T					
531H11	0.017	0.013						F454Y		
532H1	0.018	0.015				A429V				
534C7	0.016	0.020							E502G	
1032B9	0.010	0.017								T505S
1044C9	0.022	0.020			I238T					
pBC11[b]	0.013	0.003								

[a] 750 μM creosol was used to determine the activity of the VAO mutants in the cell extracts.

[b] Wild-type VAO.

Table III Steady-state kinetic paramaters of VAO and the mutants in 50 mM potassium phosphate (pH 7.5) at 25 ºC.

Substrate	Wild-type[a]		Ile238Thr[a]		Phe454Tyr[a]		Glu502Gly[a]		Thr505Ser[a]	
	k'_{cat} s^{-1}	K'_m μM	k'_{cat} s^{-1}	K'_m μM	k'_{cat} s^{-1}	K'_m μM	k'_{cat} s^{-1}	K'_m μM	k'_{cat} s^{-1}	K'_m μM
creosol	0.020	20	0.17	41	0.14	13	0.10	27	0.12	31
2-methyl-*p*-cresol	0.031	21	0.063	17	0.032	6	0.019	7	0.025	7
2-amino-*p*-cresol	0.017	123	0.079	118	0.082	167	0.099	200	0.087	254
p-cresol	0.005	31	<0.001	n.d.	<0.001	n.d.	<0.001	n.d.	<0.001	n.d.
vanillyl alcohol	1.6	75	0.39	7	0.25	7	0.22	51	0.21	6
4-(methoxymethyl)phenol	3.1	58	2.1	51	2.1	54	1.1	64	2.3	33
eugenol	14	2	0.8	8	0.50	3	0.17	5	0.65	0.8

[a] Standard errors were less than 15 %.

Table IV Steady-state kinetic paramaters of VAO and the mutants in 50 mM glycine/potassium hydroxide (pH 10) at 25 ºC.

Substrate	Wild-type[a]		Ile238Thr[a]		Phe454Tyr[a]		Glu502Gly[a]		Thr505Ser[a]	
	k'_{cat} s^{-1}	K'_m μM	k'_{cat} s^{-1}	K'_m μM	k'_{cat} s^{-1}	K'_m μM	k'_{cat} s^{-1}	K'_m μM	k'_{cat} s^{-1}	K'_m μM
creosol	0.005	2	0.07	1	0.10	2	0.09	<1	0.10	1
2-methyl-*p*-cresol	0.002	n.d.	0.02	<1	0.01	<1	0.028	1	0.023	<1
2-amino-*p*-cresol	0.001	n.d.	0.086	50	0.047	64	0.076	43	0.046	29
p-cresol	<0.001	n.d.	<0.001	n.d.	<0.001	n.d.	<0.001	n.d.	<0.001	n.d.
vanillyl alcohol	2.4	189	1.4	22	0.71	15	0.30	10	0.67	10
4-(methoxymethyl)phenol	3.9	110	3.0	20	3.4	23	1.2	4	3.6	14
eugenol	39	19	0.60	0.2	0.23	0.8	0.10	<0.2	0.55	2

[a] Standard errors were less than 15 %.

Table V Stopped-flow kinetic results of the reduction of VAO by creosol in 50 mM potassium phosphate (pH 7.5) or 50 mM glycine/potassium hydroxide (pH 10) at 25 ºC.

Enzyme	pH 7.5[a]		
	K_d (k_{-1}/k_1) μM	k_2 s^{-1}	k_{-2} s^{-1}
wild-type	188	0.57	0.18
Phe454Tyr	55	0.25	0.24
Thr505Ser	286	0.36	0.18
	pH 10[a]		
wild-type	336	1.00	0.07
Phe454Tyr	61	1.83	0.07
Thr505Ser	126	0.96	0.59

[a] Standard errors were less than 10 %.

Table VI Redox-state of the FAD cofactor in VAO during turnover of creosol in 50 mM potassium phosphate (pH 7.5) or 50 mM glycine/potassium hydrochloride (pH 10) at 25 ºC.

	FAD redox-state (% FAD_{ox})[a]	
Enzyme	pH 7.5	pH 10
Wild-type	47	12
Ile238Thr	58	24
Phe454Tyr	55	32
Glu502Gly	45	32
Thr505Ser	66	28

[a] Standard errors were less than 14 %.

Fig. 1. **Two-step conversion of creosol by VAO**. The initial aromatic product vanillyl alcohol is converted in a second catalytic cycle to vanillin.

Fig. 2 **Reduction of Thr505Ser VAO by creosol**. 2.5 μM Thr505Ser was mixed anaerobically with varying concentrations of creosol in 50 mM potassium phosphate (pH 7.5) at 25 ºC. FAD reduction was followed at 439 nm. The finite value at zero substrate concentration represent k_{-2}. The inset displays the double-reciprocal plot of the kinetic data corrected for k_{-2}.

Fig. 3 **Time-dependent fluorescence emission changes upon reaction of VAO (mutants) with creosol.** 8 μM enzyme was mixed with 200 μM creosol in 50 mM potassium phosphate (pH 7.5) or glycine/potassium hydroxide (pH 10) at 25 ºC. The excitation wavelength was 360 nm. Spectra were recorded after 10 s (a) and at 1 (b) and 5 min (c). *A*, wild-type VAO pH 7.5; *B*, wild-type VAO pH 10; *C*, Phe454Tyr pH 7.5; *D*, Phe454Tyr pH 10; *E*, Thr505Ser pH 7.5 and *F*, Thr505Ser pH 10. For comparison, the fluorescence emission spectra of 200 μM vanillin (d), 8 μM free enzyme (e), and wild-type VAO: *p*-cresol adduct (f) are shown in Fig. 4*B*. The fluorescence properties of Ile238Thr and Glu502Gly were similar to Thr505Ser and Phe454Tyr, respectively.

Fig. 4 **Crystal structure of VAO monomer**. The cap domain is depicted in dark grey and the FAD-binding domain in light grey. The FAD and isoeugenol are shown as ball-and-stick. The four evolved mutations each resulting in an increased reactivity towards creosol are shown as ball-and-stick. The figure was prepared using MOLSCRIPT (56) and Raster3D (57).

Fig. 5 **Structural comparison of wild-type VAO with VAO mutants and PCMH.** *A*, superposition of isoeugenol-complexed wild-type VAO (light grey) and isoeugenol-complexed Phe454Tyr (dark grey). *B*, Superposition of isoeugenol-complexed wild-type VAO (light grey) and isoeugenol-complexed Thr505Ser (dark grey). *C*, Superposition of *p*-cresol-complexed wild-type VAO (light gray) and *p*-cresol-complexed PCMH (dark grey). The figures were prepared with MOLSCRIPT (56) and Raster3D (57).

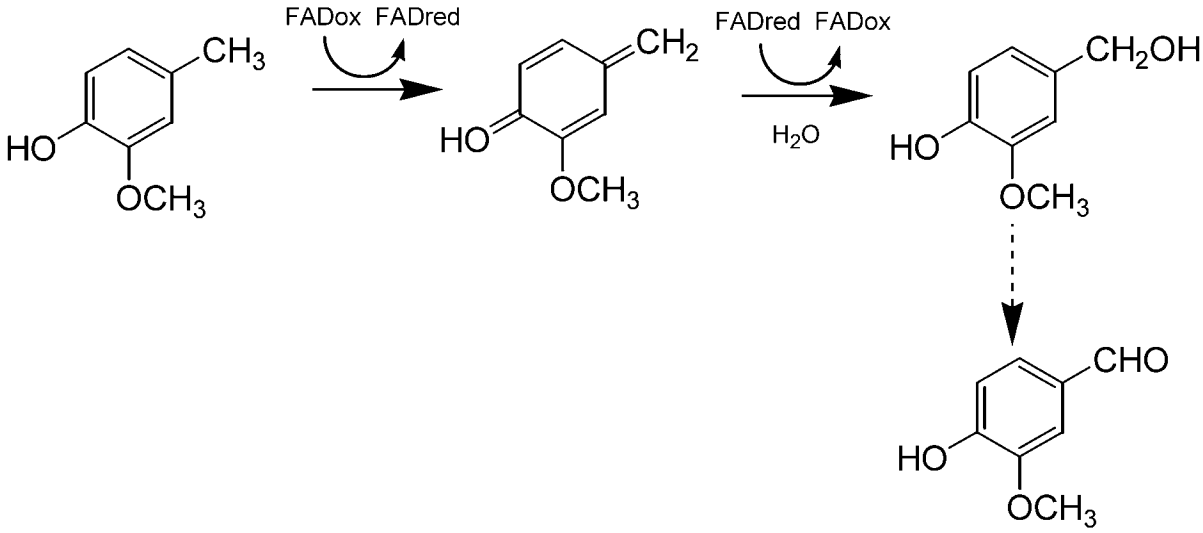

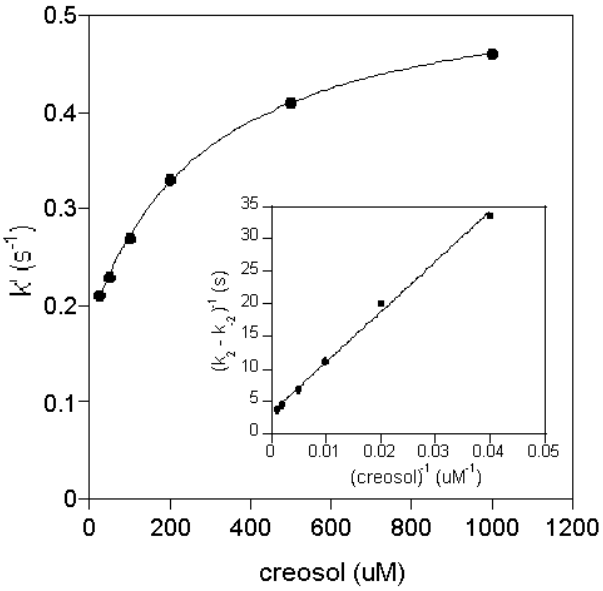

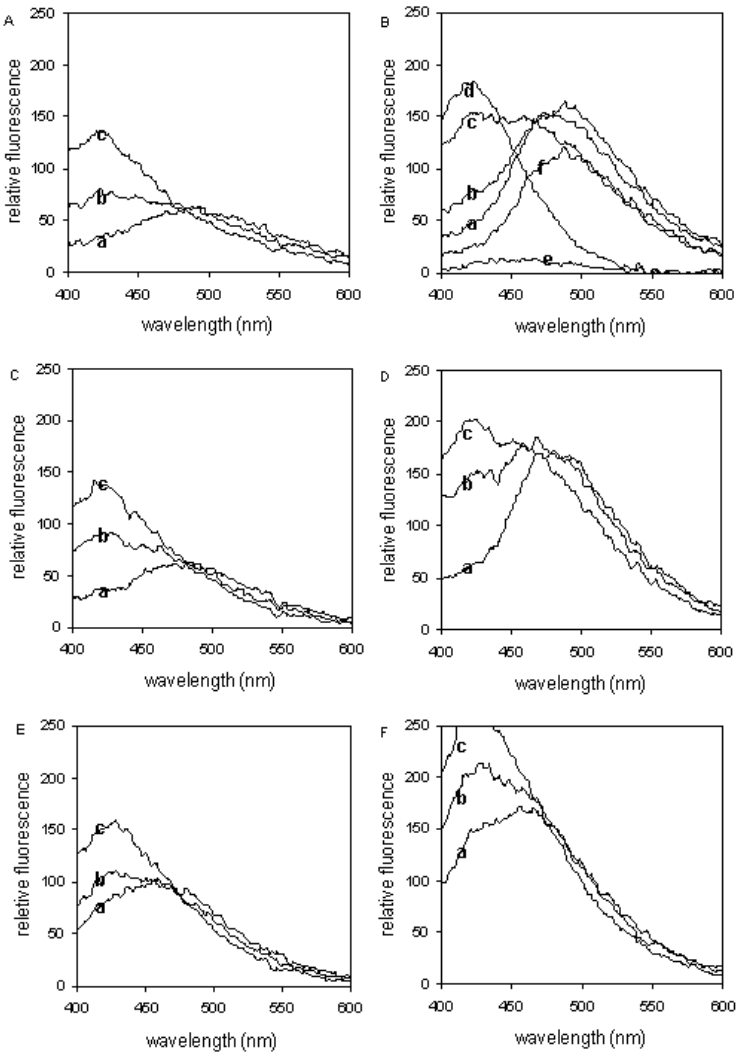

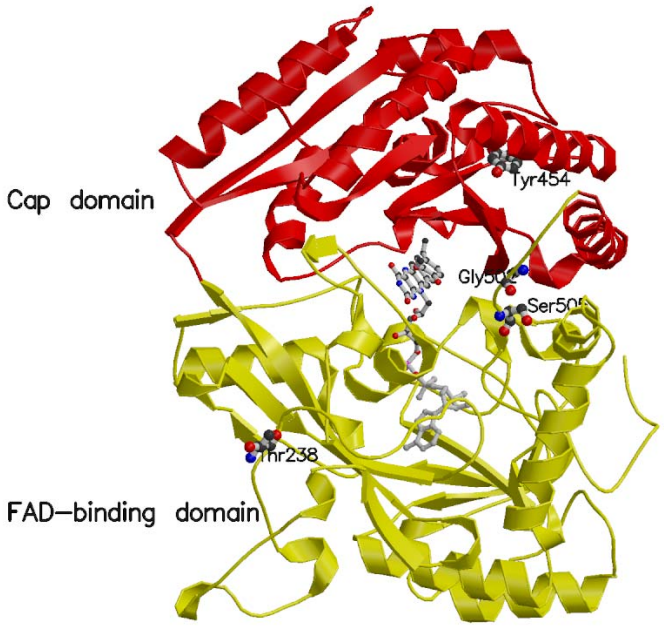

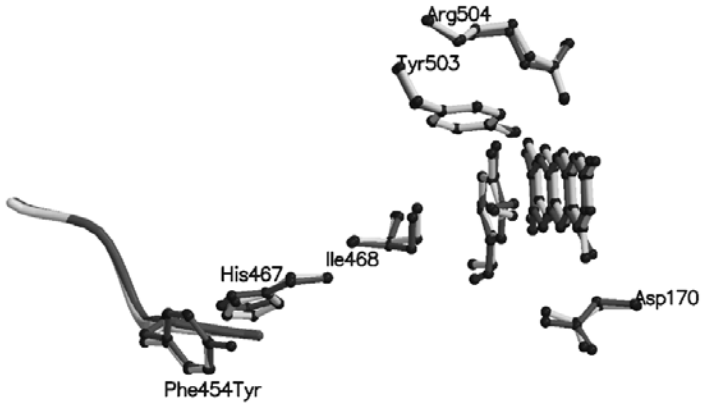

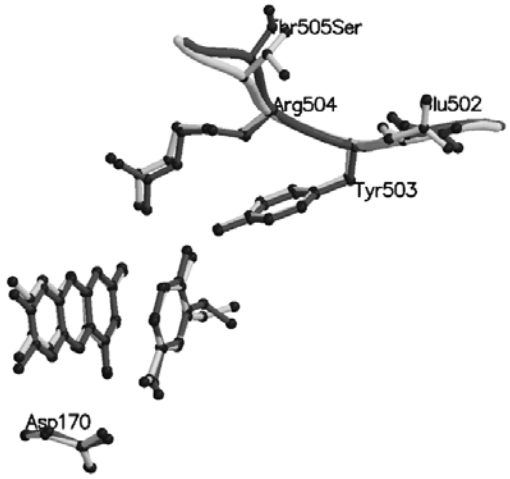

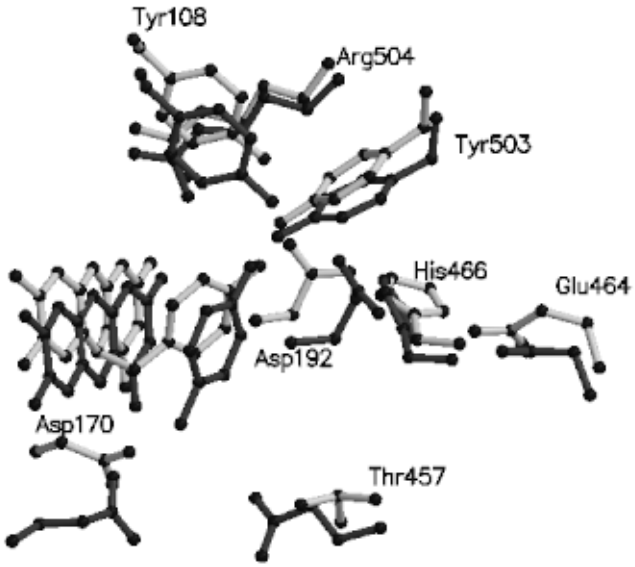

Laboratory-evolved vanillyl-alcohol oxidase produces natural vanillin

Robert H. H. van den Heuvel, Willy A. M. van den Berg, Stefano Rovida and Willem J. H. van Berkel

J. Biol. Chem. published online May 28, 2004
